JOC Featured Article

Hydrolysis and Photolysis of 4-Acetoxy-4-(benzothiazol-2-yl)-2,5-cyclohexadien-1-one, a Model Anti-Tumor Quinol Ester

Yue-Ting Wang,[†] Kyoung Joo Jin,[†] Lauren R. Myers,[†] Stephen A. Glover,[‡] and Michael Novak*,[†]

Department of Chemistry and Biochemistry, Miami University, Oxford, Ohio 45056, and Division of Chemistry, School of Science and Technology, University of New England, Armidale, 2351, New South Wales, Australia

novakm@muohio.edu

Received April 23, 2009

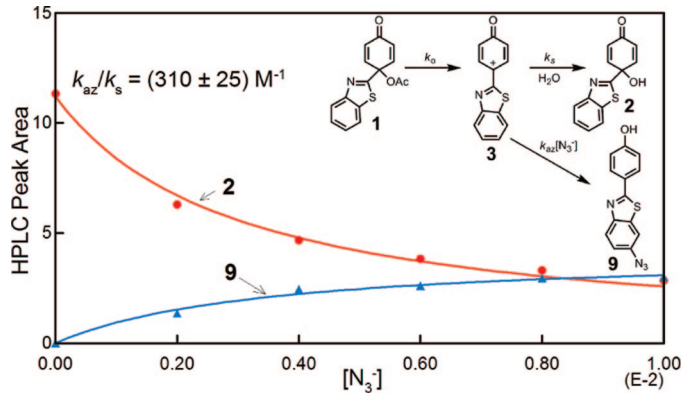

4-Acetoxy-4-(benzothiazol-2-yl)-2,5-cyclohexadien-1-one, **1**, a quinol derivative that exhibits significant anti-tumor activity against human breast, colon, and renal cancer cell lines, undergoes hydrolysis in aqueous solution to generate an oxenium ion intermediate, **3**, that is selectively trapped by N_3^- in an aqueous environment. The 4-(benzothiazol-2-yl) substituent slows the rate of ionization of **1** compared to analogues with 4-phenyl or 4-(*p*-tolyl) substituents, **4a** or **4b**. However, once generated, **3** is somewhat more selective than the 4-phenyl-substituted cation **5a**. Calculations performed at the B3LYP/6-31G(d) level agree that the 4-(benzothiazol-2-yl) substituent does significantly stabilize **3**. The structure of the major isolated azide adduct, 4-(6-azidobenzothiazol-2-yl)phenol, **9**, confirms that the positive charge is highly delocalized in **3**. The results of hydrolysis of **1** show that the 4-(benzothiazol-2-yl) substituent has a significant inductive electron-withdrawing effect as well as a significant resonance effect that is electron-donating. Photolysis of **1** in aqueous solution generates the quinol **2** as one of several photolysis products. The presence of the quinol suggests that photolysis also leads, in part, to generation of **3**, but photoionization of **1** is significantly less efficient than is the case for the esters **4a** and **4b**. This study proves that **3** is generated by ionization of **1** in an aqueous environment. A significant number of other 2-benzothiazole derivatives that are not quinols, including ring-substituted derivatives of 2-(4-aminophenyl)benzothiazole **15**, are under development as anti-tumor agents as well. The possible generation of the reactive intermediate **17** by hydrolysis of the putative metabolite **16** is under investigation.

Introduction

The 4-(benzothiazol-2-yl)-substituted quinol ester **1** and the parent quinol **2** have been shown to have activity against the human colon cancer cell lines HCT 116 and HT 29 as well as against the breast cancer cell lines MCF-7 and MDA 468 with IC_{50} values at the 40−800 nM level.[1,2] Selective activity for

[†] Miami University.
[‡] University of New England.

(1) Wells, G.; Bradshaw, T. D.; Diana, P.; Seaton, A.; Shi, D.-F.; Westwell, A. D.; Stevens, M. F. G. *Bioorg. Med. Chem. Lett.* **2000**, *10*, 513–515.

10.1021/jo9008436 CCC: $40.75 © 2009 American Chemical Society
Published on Web 05/28/2009

both compounds against renal and colon cancer cell lines was discovered on the NCI Developmental Therapeutics Screening Program in vitro screen against 60 human cancer cell lines.[2] In vivo activity against the human renal tumor xenograft RXF 944LX in mice was also demonstrated.[2] Structurally related quinol derivatives, including some indol-2-yl and benzimidazol-2-yl derivatives, have also shown activity against breast, colon, and renal cancer cell lines.[3−5] Thioredoxin has been identified as one target of **2** and related quinols.[6,7] Irreversible binding of **2** to the protein has been demonstrated, but the chemical nature of the reaction has not been studied in detail.[6] Other possible protein targets of **2** have been identified, but nonprotein targets have not be elucidated.[8]

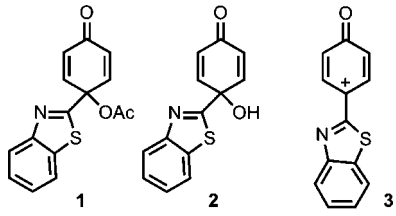

The irreversible inhibition of thioredoxin is thought to occur by a double conjugate addition of two cysteine residues in the active site of the protein directly on **2**.[6] However, our experience with quinols closely related to **2** shows that they are not very reactive with nucleophiles.[9−13] Quinol esters similar to **1** have recently been shown to generate oxenium ions in aqueous solution.[9−13] These cations are reactive with water but still react very selectively with strong nucleophiles in an aqueous environment.[9−13] An alternative hypothesis to the direct reaction of **2** with biological nucleophiles would be the reaction of the oxenium ion **3**, generated by ionization of **1**, a likely metabolite of **2**, with these nucleophiles. This hypothesis relies on the ability of the benzothiazol-2-yl group to stabilize **3** by delocalization of the positive charge. Qualitatively, this seems likely, and calculations performed at the B3LYP/6-31G(d) level presented herein support that assumption. However, the benzothiazol-2-yl group is a known inductive electron-withdrawing substituent with a σ_p of 0.29 determined from its effect on the ionization constants of substituted benzoic acids.[14,15] This substituent may cause a significant deceleration of the ionization process that has previously been shown to be sensitive to electron-withdrawing substituents.[11] It is not clear which effect of the benzothiazol-2-yl group would be dominant in the chemistry of **1**. If the electron-withdrawing inductive effect destabilizes the transition state leading to ionization sufficiently, it is possible that the chemistry of **1** is dominated by reactions that do not generate **3**. On the other hand, if the transition state for ionization is sufficiently cation-like, the ability of the 2-benzothiazolyl group to delocalize the positive charge via resonance may dominate.

In this paper, we provide evidence that both of the expected electronic properties of the benzothiazol-2-yl group play a role in the chemistry of **1**. Ionization to generate **3** does occur, although the rate of the reaction is significantly slower than that of related quinol esters **4a** and **4b** with electron-donating 4-aryl substituents. Once generated, **3** is a fairly selective ion that is readily trapped by N_3^- at $[N_3^-] < 0.05$ M.

Previously, we have shown that **4a** and **4b** can be photolyzed in aqueous solution to generate the oxenium ions **5a** and **5b**, although this process occurs in competition with homolysis to generate the corresponding radicals **6a** and **6b**.[12,13] The homolysis occurs exclusively in the less polar solvent CH_3CN.[13] Photolysis products of **1** in aqueous solution and in CH_3CN can also be explained, in part, by a combination of heterolysis and homolysis, although some products appear to be generated by other processes.

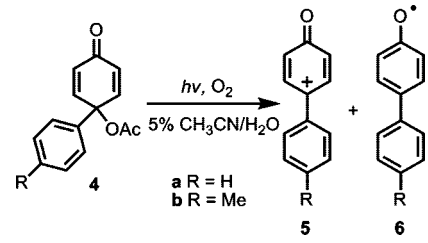

Results and Discussion

We have previously used ground state singlet energies of aryloxenium ions to calculate ΔE of isodesmic reactions such as eq 1.[11,16] We have successfully correlated these ΔE with the experimental lifetimes of 4′-substituted biphenylyloxenium ions.[11] Similar calculations have been used to understand the properties of other aryloxenium and arylnitrenium ions.[9,10,16,17] ΔE of eq 1 measures the thermodynamic stability of **5a** and **5b** relative to their respective hydration products **7a** and **7b**. At the pBP/DN*//HF/6-31G(d) and BP/6-31G(d)//HF/6-31G(d) levels, ΔE for eq 1 without ZPE corrections is 3.41 and 5.46 kcal/mol, respectively.[11] The calculated stabilization of **5b** relative to **5a** agrees well with the observed ca. 14-fold greater lifetime of **5b** in aqueous solution at 30 °C (170 ns for **5b** vs 12 ns for **5a**) in a correlation of log(lifetime) versus ΔE for four 4′-substituted biphenylyloxenium ions.[11] A similar correlation of log(lifetime) versus ΔE was observed for a much larger series of arylnitrenium ions and their hydration products at the HF/6-31G(d)//3-21G level of theory.[17]

At the B3LYP/6-31G(d) level of DFT, oxenium ions **3**, **5a**, and **5b** all have singlet ground states. Their corresponding triplet

(2) Wells, G.; Berry, J. M.; Bradshaw, T. D.; Burger, A. M.; Wang, B.; Westwell, A. D.; Stevens, M. F. G. *J. Med. Chem.* **2003**, *46*, 532–541.
(3) Berry, J. M.; Bradshaw, T. D.; Fichtner, I.; Ren, R.; Schwalbe, C. H.; Wells, G.; Chew, E.-H.; Stevens, M. F. G.; Westwell, A. D. *J. Med. Chem.* **2005**, *48*, 639–644.
(4) McCarroll, A. J.; Bradshaw, T. D.; Westwell, A. D.; Matthews, C. S.; Stevens, M. F. G. *J. Med. Chem.* **2007**, *50*, 1707–1710.
(5) Lion, C. J.; Matthews, C. S.; Wells, G.; Bradshaw, T. D.; Stevens, M. F. G.; Westwell, A. D. *Bioorg. Med. Chem. Lett.* **2006**, *16*, 5005–5008.
(6) Bradshaw, T. D.; Matthews, C. S.; Cookson, J.; Chew, E.-H.; Shah, M.; Bailey, K.; Monks, A.; Harris, E.; Westwell, A. D.; Wells, G.; Laughton, C. A.; Stevens, M. F. G. *Cancer Res.* **2005**, *65*, 3911–3919.
(7) Mukherjee, A.; Huber, K.; Evans, H.; Lakhani, N.; Martin, S. *Br. J. Pharmacol.* **2007**, *151*, 1167–1175.
(8) Chew, E.-H.; Matthews, C. S.; Zhang, J.; McCarroll, A. J.; Hagen, T.; Stevens, M. F. G.; Westwell, A. D.; Bradshaw, T. D. *Biochem. Biophys. Res. Commun.* **2006**, *346*, 242–251.
(9) Novak, M.; Glover, S. A. *J. Am. Chem. Soc.* **2004**, *126*, 7748–7749.
(10) Novak, M.; Glover, S. A. *J. Am. Chem. Soc.* **2005**, *127*, 8090–8097.
(11) Novak, M.; Poturalski, M. J.; Johnson, W. L.; Jones, M. P.; Wang, Y.-T.; Glover, S. A. *J. Org. Chem.* **2006**, *71*, 3778–3785.
(12) Wang, Y.-T.; Wang, J.; Platz, M. S.; Novak, M. *J. Am. Chem. Soc.* **2007**, *129*, 14566–14567.
(13) Wang, Y.-T.; Jin, K. J.; Leopold, S. H.; Wang, J.; Peng, H.-L.; Platz, M. S.; Xue, J.; Phillips, D. L.; Glover, S. A.; Novak, M. *J. Am. Chem. Soc.* **2008**, *130*, 16021–16030.
(14) Bystrov, V. F.; Belaya, Zh. N.; Gruz, B. E.; Syrova, G. P.; Tolmachev, A. I.; Shulezhko, L. M.; Yagupol'skii, L. M. *Zh. Obshchei Khimii* **1968**, *38*, 1001–1005.
(15) Durmis, J.; Karvas, M.; Manasek, Z. *Collect. Czech. Chem. Commun.* **1973**, *38*, 215–223.
(16) Glover, S. A.; Novak, M. *Can. J. Chem.* **2005**, *83*, 1372–1381.
(17) Novak, M.; Lin, J. *J. Org. Chem.* **1999**, *64*, 6032–6040.

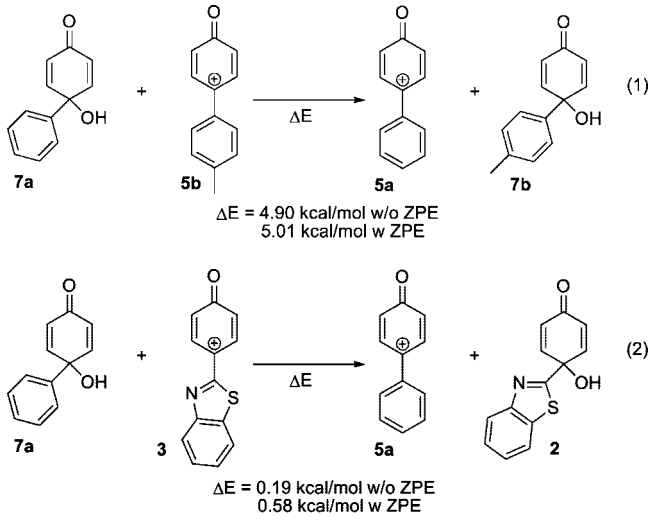

states are computed to be 22.3, 22.3, and 23.2 kcal/mol, respectively, higher in energy in keeping with T−S_0 gaps computed previously by DFT for phenyl- and 4-methylphenyloxenium ions.[16] Using S_0 energies, the energetics of the isodesmic reactions of eq 1 and eq 2 were compared at the B3LYP/6-31G(d) level with and without ZPE corrections. The results are shown in the equations. ΔE calculated at this level for eq 1 is comparable to the results previously obtained at the pBP/DN*//HF/6-31G(d) and BP/6-31G(d)//HF/6-31G(d) levels. The results for the isodesmic reaction of eq 2 suggest that the 4-(benzothiazol-2-yl) substituent is similar to the 4-Ph substituent in its ability to stabilize an aryloxenium ion. If **3** can be generated by ionization of **1**, it should have a lifetime long enough for it to be detected by N_3^- trapping.[9−13]

This conclusion is supported by the computed properties of **3**, **5a**, and **5b**. B3LYP/6-31G(d) charges and bond lengths for **5b** have recently been reported along with its computed and experimental vibrational spectrum.[13] Corresponding data for **3** and **5a** are given in Figure 1a,b. All three ions exhibit 2,5-cyclohexadien-1-one-4-yl cationic character. The carbonyl stretch frequency for **5b** has been calculated at 1672 cm^{-1} in the gas phase. This correlates with that observed by time-resolved resonance Raman spectroscopy (1635 cm^{-1} in aqueous solution).[13] **3** and **5a** are computed to have similar scaled carbonyl stretch vibrations at 1663 and 1672 cm^{-1}.[18] In all three ions, the positive charge is essentially on the 4-position and on the 4-aryl substituent rather than on the oxygen atom.

The dipole moments for **3**, **5a**, and **5b** are 4.00, 4.29, and 4.45 D, respectively, and are aligned largely along the molecular axes toward the substituent ring. The total Mulliken charges on the substituent aryl groups in **3** and **5a** are, respectively, +0.49 and +0.47, while the corresponding charge on the *p*-tolyl group in **5b** is +0.52.[13] Though slightly less efficient than 4-(*p*-tolyl), both 4-phenyl and 4-(benzothiazol-2-yl) have a similar capacity to delocalize the positive charge away from the 4-position of the aryloxenium ion. Interestingly, B3LYP/6-31G(d) computes **5a** and **5b** to be slightly twisted, with inter-ring dihedral angles of 19 and 14°, respectively, while **3** is completely planar. The inter-ring bond in **3** (1.414 Å) is also shorter than that in **5a** and **5b** (1.432 and 1.427 Å, respectively).[13] These differences probably reflect the reduced steric demand of the heteroatoms in **3** as opposed to CH at C-2′ and C-6′ in **5a** and **5b** rather than an enhanced resonance interaction with the benzothiazole system.

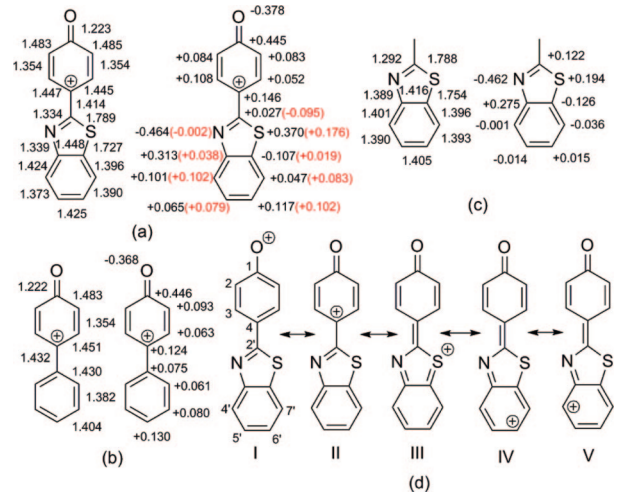

FIGURE 1. Bond lengths and charges computed at the B3LYP/6-31G(d) level for (a) **3**, (b) **5a**, and (c) 2-methylbenzothiazole (charges on H summed into the heavy atoms); (d) resonance forms for **3**. Data in red correspond to charge differences between atoms in **3** and those of the corresponding atoms in 2-methylbenzothiazole.

Like **5b**,[13] delocalization into the 4-phenyl ring of **5a** is evidenced by strong bond alternation (Figure 1b). Positive charge is greatest at C-2, C-4, and C-4′, the known sites of trapping by water and azide.[9,10] Delocalization throughout **3** is also evident from a comparison of the ground state structures of **3** with 2-methylbenzothiazole computed at the same level. While the carbon−carbon bond lengths in 2-methylbenzothiazole are similar (Figure 1c), in **3**, they show a high degree of bond length alternation (Figure 1a). Notably, the ring-junction carbon−carbon bond is 0.032 Å longer in the oxenium ion. This, together with significant lengthening of the N−(C-2′) bond, corresponding contraction in the N−(C-3a′) and S−(C-7a′) bonds, as well as a charge increase on S of +0.176, points to a strong contribution of resonance form III in Figure 1d. Substantial increases in charge at C-4′ and C-6′ relative to 2-methylbenzothiazole are also evident, pointing to resonance representations IV and V.

By analogy to **5a**, in which water attacks at C-4 and azide reacts at C-2 and C-4′,[9,10] nucleophilic attack on **3** should occur at C-2 and C-4 of the phenyl ring and at C-4′ and C-6′ on the distal benzothiazole group. All these positions contribute strongly to the LUMO of **3** shown in Figure 2.

The quinol ester **1** was synthesized from the oxidation of the corresponding phenol **8** by phenyliodonium diacetate (PIDA) in AcOH in ca. 20% yield. This procedure has been applied to synthesize other quinol esters in low to moderate yields.[9,11] **1** is stable enough in the dark to be purified by radial chromatography on silica gel. Synthesis and characterization of all compounds is presented in the Experimental Section, and ^1H and ^{13}CNMR spectra are reported in the Supporting Information.

Kinetics of decomposition of **1** were measured at 80 °C in $HClO_4$ solutions (pH < 3.0) or in HCO_2H/$NaHCO_2$, AcOH/AcONa, NaH_2PO_4/Na_2HPO_4 buffers (5 vol % CH_3CN−H_2O, μ = 0.5 ($NaClO_4$)) by monitoring changes in UV absorbance as a function of time. All reactions were performed with an initial ester concentration of ca. 5×10^{-5} M. Absorbance versus time data were fit to a first-order or a consecutive first-order rate equation. Rate constants taken at a minimum of three wave-

(18) Scott, A. P.; Radom, L. *J. Phys. Chem.* **1996**, *100*, 16502–16513.

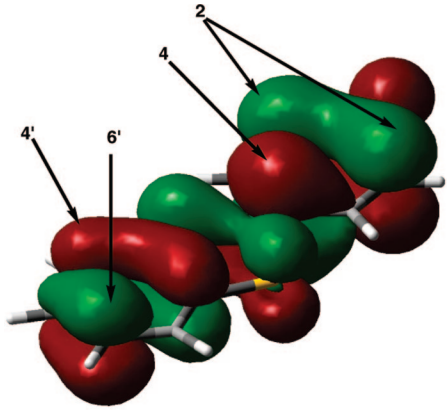

FIGURE 2. LUMO of **3** at the B3LYP/6-31G(d) level. Arrows denote likely positions for nucleophilic attack.

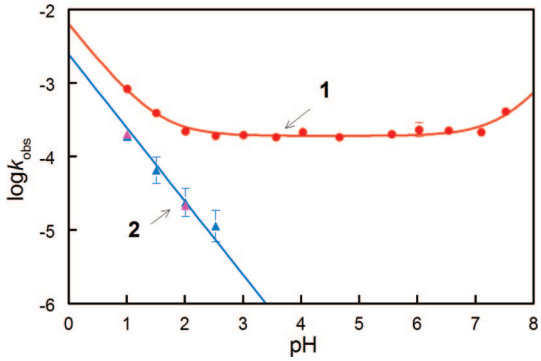

FIGURE 3. The pH dependence of the decomposition of **1** and **2** at 80 °C. Red circles correspond to the hydrolysis rate constants for decomposition of **1**; blue triangles correspond to acid-catalyzed decomposition of **2** determined by consecutive first-order fitting of the rate data for **1**; magenta triangles correspond to directly measured rate constants for acid-catalyzed decomposition of authentic **2**. Data were fit to eqs 3 and 4 as described in the text.

lengths were averaged at each pH. Consecutive first-order reactions were found only at pH < 3.0. Under these acidic conditions, one rate constant was found to be experimentally equivalent to the rate constant for acid-catalyzed decomposition of **2**, the major hydrolysis product of **1**. The absorbance versus time data for the decomposition of authentic **2** at pH < 3.0 fit a standard first-order rate equation well. All k_{obs} for **1** and **2** are provided in the Supporting Information. The pH dependence of the decomposition of **1** and **2** is summarized in Figure 3. The k_{obs} for decomposition of **1** at pH 1.0−7.5 was fit to the rate law of eq 3. The k_{obs} for decomposition of **2** at pH 1.0−2.5 was fit to the rate law of eq 4. Both **1** and **2** could be protonated at N-3′ in sufficiently acidic solution, but neither the kinetic data nor UV spectra of these compounds indicate that protonation occurs at pH ≥ 1.0.

$$k_{obs}^{1} = k_{o}^{1} + k_{H}^{1}[H^{+}] + k_{OH}^{1}[OH^{-}] \quad (3)$$

$$k_{obs}^{2} = k_{H}^{2}[H^{+}] \quad (4)$$

1 exhibits pH-independent decomposition kinetics from pH 2 to 7 and pH-dependent decomposition at pH < 2 and pH > 7. Three rate constants, k_o^1, k_H^1, and k_{OH}^1, were used to fit the rate data: k_o^1 corresponds to the pH-independent decomposition pathway that is dominant over a wide pH range, while k_H^1 and k_{OH}^1 describe acid-catalyzed and base-catalyzed decomposition pathways, respectively. The first two rate terms of eq 3 are consistent with what we observed for the oxenium ion precursors **4a** and **4b**.[9,11] For these two esters, the processes governed by both k_o and k_H involve formation of the cations **5a** and **5b**.[9−11] However, no rate term corresponding to k_{OH} was observed for **4a** and **4b** in basic phosphate buffers.[9,11] Quinol **2** decomposes slowly through an acid-catalyzed pathway governed by k_H^2. This process became exceedingly slow at pH > 3.0, so the decomposition of **2** no longer interfered with the measurement of the kinetics of decomposition of **1** except at pH > 7.0. HPLC examination and repetitive wavelength scans showed that **2** slowly decomposes in basic phosphate buffers, but its decomposition kinetics were not examined in detail under these conditions. Negligible absorbance changes occurred for the decomposition of **2** in phosphate buffers in the range from 250 to 270 nm, so it was possible to monitor the decomposition kinetics of **1** in this wavelength range without interference from the much slower decomposition of **2**. Rate constants derived from the fits to eq 3 and eq 4 for the decomposition of **1** and **2** are reported in Table 1 with some comparisons to **4a** and **4b**.

TABLE 1. Derived Rate Parameters for the Decomposition of 1 and 2 and 4a and 4b

	T (°C)	k_o (s^{-1})	k_H (M^{-1} s^{-1})	k_{OH} (M^{-1} s^{-1})
1	80	(1.91 ± 0.08) × 10^{-4}	(6.2 ± 0.8) × 10^{-3}	(5.5 ± 1.2) × 10^{2}
2	80		(2.5 ± 0.4) × 10^{-3}	
4a[a,c]	30	(2.50 ± 0.05) × 10^{-5}	(1.45 ± 0.08) × 10^{-3}	
4b[b,c]	30	(1.02 ± 0.01) × 10^{-3}	(1.95 ± 0.08) × 10^{-2}	
4a[d]	80	(4.5 ± 0.4) × 10^{-3}		
4b[e]	80	(1.0 ± 0.1) × 10^{-1}		

[a] Data from ref 9. [b] Data from ref 11. [c] Reaction conditions, except temperature, identical to **1**. [d] Extrapolated to 80 °C from data taken in the 30 to 70 °C range. [e] Extrapolated to 80 °C from data taken in the 20 to 40 °C range.

Comparison of k_o^1 to the corresponding rate constants for **4a** and **4b** clearly shows that the rate of uncatalyzed decomposition of **1** is significantly depressed compared to other quinol esters that generate oxenium ions. At 80 °C, the uncatalyzed decomposition of **1** occurs ca. 24-fold more slowly than the decomposition of **4a** and ca. 520-fold more slowly than **4b**, while the N_3^- trapping data shown below indicate that **1** does generate **3**. Therefore, the benzothiazol-2-yl group is clearly acting as an electron-withdrawing group that destabilizes the transition state for ionization and decreases the rate of ionization. The base-catalyzed term k_{OH} was not observed for **4a** or **4b** at pH < 8.0.[9,11] If k_{OH} is about the same magnitude for **4a** and **4b** at 80 °C as k_{OH}^1, it would not be possible to detect the base-catalyzed reaction for **4a** below ca. pH 9.2 or for **4b** below pH 10.6 because of the larger magnitudes of k_o for these compounds compared to **1**. Since it is probable that the base-catalyzed hydrolysis of **1** is accelerated by the electron-withdrawing benzothiazol-2-yl group, it is likely that the pH estimates for the onset of observable base-catalyzed hydrolysis of **4a** and **4b** are lower limits.

The HPLC examination of the decomposition of **1** showed that, at pH > 3.0 in the absence of any nucleophile other than H_2O, only one significant product was detected. This product was isolated from the hydrolysis of **1** in pH 4.61 acetate buffer at 80 °C in 71% yield and was identified as the quinol **2**. At pH < 3.0, **2** decomposes into a new material that has nearly the same HPLC retention time as **2**. The new material can be differentiated from **2** by its different absorbance characteristics from **2** at the two wavelengths used to monitor the HPLC

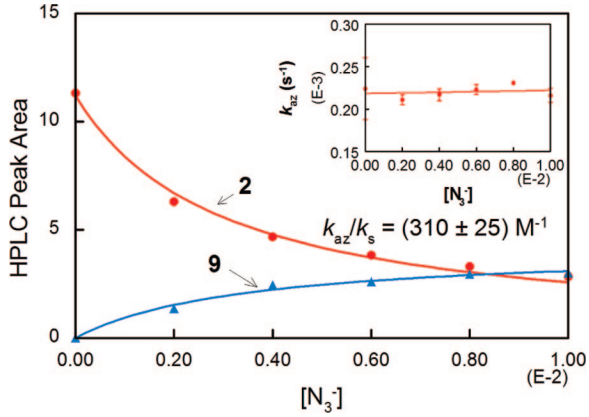

FIGURE 4. Azide trapping experiments for **1** performed at pH 6.5 in 0.02 M phosphate buffer. Data were fit by least-squares procedures to the standard "azide clock" equations as described in the text. Inset: Rate constants for decomposition of **1** in the presence of N_3^- in pH 6.5 0.02 M phosphate buffer.

chromatography (212 and 235 nm). The same material was also detected by HPLC as the final product of the hydrolysis **1** at pH < 3.0. This material was not isolated, but quinols similar to **2** have previously been shown to undergo dienone−phenol rearrangements under these conditions.[10,19] The yield of **2** determined by HPLC quantification in buffers from pH 3.5 to 6.5 after 8 half-lives (ca. 8 h) of the hydrolysis of **1** is somewhat higher than the isolated yield at pH 4.6 at ca. 85−90%. In more basic phosphate buffers, authentic **2** slowly decomposes, so its yield determined after the same reaction time is lower. For example, the yield of **2** from the hydrolysis reaction of **1** in pH 7.1 phosphate buffer determined after 8 h of reaction is somewhat lower at 72%. For this reason, the wavelengths used to monitor the decomposition kinetics of **1** in phosphate buffer at pH 7.1 and 7.5 were chosen from the wavelength range in which the decomposition of **2** did not show an absorbance change. Quinol **2** is the expected product of the reaction of the cation **3** with the aqueous solvent. Both the product and the kinetics of the hydrolysis reaction of **1** are consistent with what we have observed for other quinol esters that yield oxenium ion intermediates,[9−13] but these data do not require the intermediacy of an oxenium ion since **2** would also be the product of an ordinary ester hydrolysis.

Results of azide trapping experiments performed on **1** in phosphate buffer at pH 6.5 are summarized in Figure 4. In the presence of N_3^-, the hydrolysis product **2** was replaced by the azide trapping adduct **9** without an apparent increase in the overall rate constant for decomposition of **1** (Figure 4, inset).

The N_3^- results require a two-step mechanism in which N_3^- and water compete for the same electrophilic intermediate generated in a prior rate-limiting step. The intermediate most consistent with the generation of **2** and **9** is the oxenium ion **3** (Scheme 1). Control experiments showed that the reaction between N_3^- and quinol **2** is negligible under our reaction conditions. All the loss of **2** can be attributed to the trapping of the cation **3**. There are two apparent azide trapping products detected by HPLC, but only the major one **9** was successfully isolated by multiple application of radial chromatography. The structure of **9** indicates that the positive charge in **3** is significantly delocalized into the thiazole substituent, particularly at C-6′ of the benzothiazole ring. Differing regioselectivity for

SCHEME 1. Azide Trapping during Hydrolysis of 1

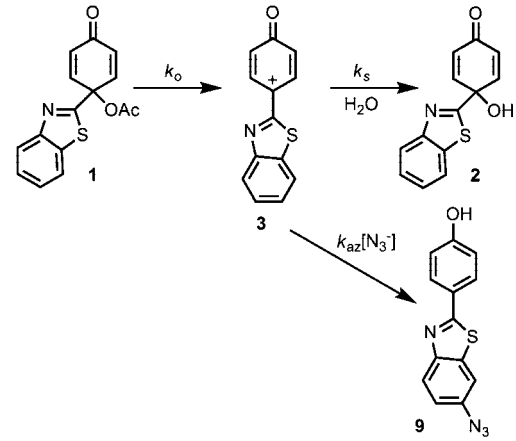

attack of H_2O and N_3^- is a common feature of both aryloxenium and arylnitrenium ions.[9−11,17,20] It is likely that N_3^- also attacks these cations, at least in part, at C-4, but these products are unstable and undergo rearrangement to more thermodynamically stable N_3^- adducts.[20] The product data obtained at different $[N_3^-]$ fit to the standard "azide clock" equations to generate k_{az}/k_s,[21,22] the ratio of the second-order rate constant for the reaction between **3** and N_3^- to the first-order rate constant for the trapping of **3** by the aqueous solvent. This ratio describes the selectivity of the intermediate toward trapping by N_3^- versus the aqueous solvent. For **3**, k_{az}/k_s is 310 ± 25 M^{-1}.

The two oxenium ions **5a** and **5b** derived from **4a** and **4b** have k_{az}/k_s of 77 and 1.0×10^3 M^{-1}, respectively, at 30 °C.[9,11] Provided that these ratios are not strongly affected by temperature, the ability of the benzothiazol-2-yl substituent to stabilize the cation appears to be between that of phenyl and *p*-tolyl substituents when they are placed at the 4-position in the aryl ring of the cation. If the reaction between the intermediate **3** and N_3^- is diffusion-limited, as is the case for other reactive oxenium and nitrenium ions,[12,23,24] k_{az} will be ca. 6.5×10^9 M^{-1} s^{-1} at 20 °C.[12] Extrapolation of k_{az} to 80 °C, based on the temperature dependence of other diffusion-controlled reactions, gives an estimate for the rate constant of ca. 1.6×10^{10} M^{-1} s^{-1}.[25,26] Then the estimated lifetime ($1/k_s$) of **3** in aqueous solution at 80 °C is ca. 20 ns. That lifetime would be expected to be longer at 30 °C, so **3** would appear to be somewhat longer lived than **5a** (ca. 12 ns) under the same conditions.[9] The differences in behavior between **3** and **5a** are small enough that the lifetimes of these two cations in aqueous solution under identical conditions are likely to be within a factor of 2 to 3 of each other.

The combination of kinetic data and azide trapping results shows that the 4-(benzothiazol-2-yl) substituent has two significantly different electronic effects. Inductive electron withdrawl dominates in destabilizing the transition state for ionization as C-4 of **1** transforms from a saturated tetrahedral carbon

(19) Vitullo, V. P.; Logue, E. A. *J. Org. Chem.* **1973**, *38*, 2265–2267.

(20) Novak, M.; Kahley, M. J.; Lin, J.; Kennedy, S. A.; James, T. G. *J. Org. Chem.* **1995**, *60*, 8294–8304.

(21) Jencks, W. P. *Acc. Chem. Res.* **1980**, *13*, 161–169.

(22) Richard, J. P.; Jencks, W. P. *J. Am. Chem. Soc.* **1982**, *104*, 4689−4691; **1982**, *104*, 4691−4692; **1984**, *106*, 1383−1396.

(23) Davidse, P. A.; Kahley, M. J.; McClellend, R. A.; Novak, M. *J. Am. Chem. Soc.* **1994**, *116*, 4513–4514.

(24) McClelland, R. A.; Davidse, P. A.; Hadzialic, G. *J. Am. Chem. Soc.* **1995**, *117*, 4173–4174.

(25) Buxton, G. V.; Elliot, A. J. *J. Chem. Soc., Faraday Trans.* **1993**, *89*, 485–488.

(26) Sehested, K.; Christensen, H. *Radiat. Phys. Chem.* **1990**, *36*, 499–500.

SCHEME 2. Photolysis Results[a]

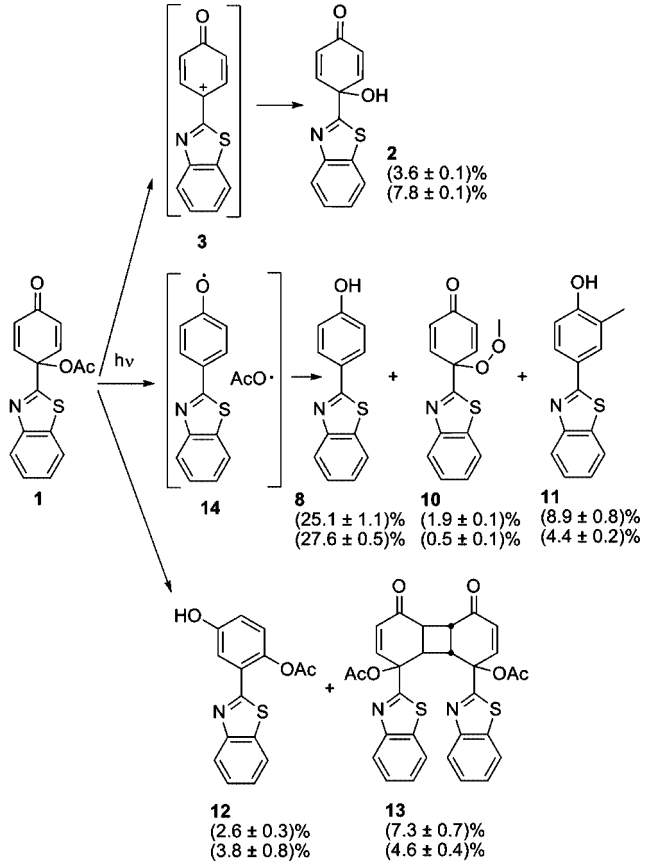

[a] Conditions: CH_3CN, O_2 (upper yields), or 20 vol % CH_3CN/H_2O, pH 5.1 acetate buffer, O_2 (lower yields), 235−280 nm.

to the trigonal carbon of **3**. Once the cation is fully formed, charge delocalization through the π-system of the 4-(benzothiazol-2-yl) substituent stabilizes the cation to a somewhat greater extent than does a 4-phenyl substituent.

Photolysis of **4a** and **4b** has previously been shown to generate both the cations **5a** and **5b** and the aryloxy radicals **6a** and **6b**.[12,13] Homolysis to form the radical is the exclusive reaction in CH_3CN, while both heterolyis and homolysis occur in aqueous solution.[13] The intermediates **5b**, **6b**, and **6a** were directly detectable by fast UV spectroscopy following nanosecond laser flash photolysis.[12,13] The cation **5a** was not directly detectable due to its short lifetime, estimated to be 12 ns from azide trapping data,[9] but **7a**, the hydration product of **5a**, was readily detected after photolysis in aqueous solution.[13]

Steady state photolysis of **1** was carried out at initial concentrations of **1** of ca. 6×10^{-4} M in oxygenated CH_3CN and 20 vol % CH_3CN/H_2O buffered with 0.02 M 1/1 HOAc/NaOAc. Some initial photoproducts (particularly **2** and **10**) were also photoreactive, so the reactions were halted when ca. 90% of **1** had been consumed. Under these conditions, photolysis of initial photoproducts was minimized, but not eliminated, so yields of **2** and **10**, in particular, are lower limits. The analogous products from photolysis of **4a** and **4b** were also photoreactive, so comparisons of relative yields can still be made.[13] HPLC analysis of reaction mixtures as photolysis proceeded showed that at least 11 initial products were generated under both photolysis conditions. Scheme 2 provides a summary of the yields of six major photoproducts that were isolated and identified. Yields are based on a combination of ^{1}H NMR integration and HPLC quantification.

Combined yields of these products account for ca. 50% of **1** that was consumed under both conditions. Some of the products (**2**, **8**, and **10**) are analogous to those isolated from the photolysis of **4a** and **4b**.[13] The products **8**, **10**, and **11** appear to be derived from the aryloxy/acetoxy radical pair **14**, while **2** is the expected hydration product of **3**.[13] A pathway for the generation of **10** from the corresponding aryloxy radical in oxygenated solutions has been presented elsewhere.[13] Combination of the aryloxy radical with methyl radical generated from decarboxylation of the acetoxy radical provides a path to **11**. Surprisingly, some **2** is generated in CH_3CN. The analogous products **7a** and **7b** were not detected during photolysis of **4a** and **4b** in CH_3CN, and **5b** could not be detected after laser flash photolysis of **4b** in CH_3CN even though **5b** is known to have a significant lifetime in aqueous solution.[13] This suggests that there may be a photolytic route from **1** to **2** in CH_3CN that does not involve **3** since this cation is less stable than **5b**. The yield of **2** significantly increases in aqueous solution. This indicates that **3** is responsible for the generation of a significant portion of **2** in aqueous solution.

The rearrangement product **12** and the dimer **13** do not appear to be derived from a cationic or radical intermediate but are likely to be derived directly from excited states of **1**. Products similar to these were not detected during photolysis of **4a** and **4b**.[12,13] The rearrangement product **12** is the expected product of a dienone−phenol photorearrangement of **1**.[27] Photodimerization of cyclohexenone derivatives usually yields *cis*−*anti*−*cis* head-to-head (H−H) or head-to-tail (H−T) dimers as the major products.[28,29] We have tentatively assigned the H−H structure to **13** based on an analysis of its ^{1}H NMR spectrum. The peak at 2.92 ppm assigned to H_a (H_a') is a simple doublet with a coupling constant of 5.0 Hz. It is coupled to the proton at 3.88 ppm assigned to H_b (H_b'). In the H−T structure H_a or H_a' would be expected to couple to both H_b and H_b' to generate a peak for H_a (H_a') that would not be a simple doublet based on observed ^{1}H NMR spectra of similar compounds.[29]

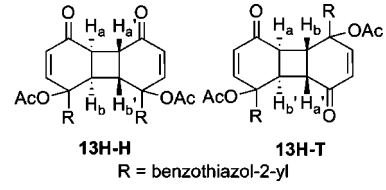

The major differences between the photolysis of **1** and those previously reported for **4a** and **4b** are the significantly lower yield of the quinol from photolysis in H_2O under similar reaction conditions (7.8% of **2**, 18% of **7a**, and 33% of **7b**) and the greater yields of products from photolysis of **1** that are not derived from cationic intermediates.[13] It appears that photoionization of **1** is suppressed compared to **4a** and **4b**. This would lead directly to a lower yield of the quinol and to greater yields of products derived from competing pathways. Suppression of photoionization is probably due to the inductive electron-withdrawing effect of the benzothiazol-2-yl group. This effect may be particularly important in the photoionization reaction

(27) Schultz, A. G.; Hardinger, S. A. *J. Org. Chem.* **1991**, *56*, 1105–1111. Schultz, A. G.; Green, N. J. *J. Am. Chem. Soc.* **1992**, *114*, 1824–1829.

(28) Lem, G.; Kaprinidis, N. A.; Schuster, D. I.; Ghatlia, N. D.; Turro, N. J. *J. Am. Chem. Soc.* **1993**, *115*, 7009–7010.

(29) Schuster, D. I.; Greenberg, M. M.; Nunez, I. M.; Tucker, P. C. *J. Org. Chem.* **1983**, *48*, 2615–2619. Yang, J.; Dewal, M. B.; Profeta, S.; Smith, M. D.; Li, Y.; Shimizu, L. S. *J. Am. Chem. Soc.* **2008**, *130*, 612–621.

since the expected vertical ionization process would initially lead to a cation with a trigonal pyramidal geometry at C-4 that would not be effectively stabilized by resonance interaction with the benzothiazol-2-yl group until it had undergone structural reorganization.

Conclusion

Azide trapping and kinetic results of the decomposition of quinol ester **1** in aqueous solution and comparison to the behavior of other quinol esters **4a** and **4b** that yield oxenium ions **5a** and **5b** prove that oxenium ion **3** is generated from uncatalyzed decomposition of **1** and that **3** is responsible for the formation of the hydration product **2** under these conditions. On the basis of the precedent of **4a**, it is also likely that the acid-catalyzed decomposition of **1** generates **3**.[10] Unlike the 4-Ph and 4-(*p*-tolyl) substituents of cations **5a** and **5b**, the 4-(benzothiazol-2-yl) substituent of **3** shows two significantly different electronic effects at different stages of the reaction. At the transition state for ionization of **1**, the inductive electron-withdrawing effect of the 4-(benzothiazol-2-yl) substituent dominates and suppresses the transformation of C-4 from a saturated tetrahedral carbon to a positively charged carbon with trigonal geometry. That makes the generation of **3** significantly slower than the generation of **5a** or **5b** at the same temperature. Once the cation is formed, the same substituent stabilizes **3** by electron delocalization through the π-system of the benzothiazole ring, confirmed by the magnitude of k_{az}/k_s and by the structure of the major azide trapping product **9**. This stabilization lies between that of the 4-phenyl and 4-(*p*-tolyl) substituents of **5a** and **5b**.

Compared to previously reported photochemistry of **4a** and **4b**, photolysis of **1** is more complicated. Besides heterolysis and homolysis routes that generate cationic transient **3** and the radical pair **14**, respectively, additional routes, including dienone−phenol photorearrangement and photodimerization, appear to be involved in the formation of rearrangement product **12** and dimer **13**. No products similar to **12** and **13** were found previously after the photolysis reactions of other oxenium ion precursors.[13] Quinol **2**, the expected product of **3** generated by photolytic heterolysis of **1**, is formed in aqueous solution but in significantly lower yield than that of **7a** and **7b** observed during photolysis of **4a** and **4b** under equivalent conditions. This suggests that the photoionization of **1** is suppressed, probably due to the inductive electron-withdrawing effect of the benzothiazol-2-yl group. A very small amount of **2** is found after photolysis of **1** in CH_3CN as well, indicating that alternative mechanisms for generation of **2** should be considered in this case. We will continue this study with emphasis on direct detection and structural characterization of **3** and the other related transients by laser flash photolysis methods.

Derivatives of 2-(4-aminophenyl)benzothiazole **15**, including one compound in phase 1 clinical trials, have been under development as anti-tumor agents.[30] Experimental data suggest that **15** is activated by N-hydroxylation and esterification, although the putative metabolite **16** had not previously been isolated.[31] It is our hypothesis that the biological activity of **15** and related derivatives is due to ionization of **16** and related compounds to generate selective nitrenium ions of general structure **17**.[32] We have recently synthesized **16** and have initiated a study of its aqueous solution chemistry that includes kinetic analysis, trapping of reactive intermediates, and possible photolytic generation of **17**. Results of these studies will be reported at a later date.[33]

TABLE 2. Wavelengths Used for Kinetic Analysis of the Decomposition of 1

reaction solution	pH	UV wavelengths monitored (nm)
$HClO_4$ solutions	1.0−2.5	212, 221, 235, 340
formate buffer	3.0−4.0	217, 257, 340
acetate buffer	4.5	217, 257, 340
phosphate buffer	5.5−6.5	222, 257, 340
phosphate buffer	7.1−7.5	250, 257, 265

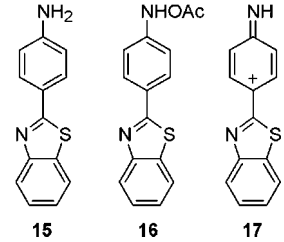

15 **16** **17**

Experimental Section

Kinetics and Product Analyses: Hydrolysis reactions were performed in 5 vol % CH_3CN-H_2O, $\mu = 0.5$ ($NaClO_4$), at 80 °C for **1** and **2**. The pH was maintained with $HClO_4$ solutions (pH < 3.0) or with $HCO_2H/NaHCO_2$, AcOH/AcONa, and NaH_2PO_4/Na_2HPO_4 buffers. All pH values were measured at ambient (20−23 °C) temperature and are uncorrected. Reactions were initiated by injecting 15 μL of a ca. 0.01 M CH_3CN solution of **1** or **2** into 3 mL of the reaction solution incubated at 80 °C for 20 min prior to the injection. The initial concentration of **1** or **2** in the reaction was ca. 5×10^{-5} M. Kinetics were monitored by changes in UV absorbance at a minimum of three wavelengths. The rate constant for each reaction was obtained as an average of all rate constants obtained at each wavelength. The wavelengths chosen to monitor the decomposition of **1** in solutions at pH 1.0−6.5 varied slightly in different reaction solutions due to slight shifts of the maximum absorbance changes observed in these solutions. In phosphate buffers at pH 7.1 and 7.5, the decomposition kinetics of **1** were monitored at wavelengths chosen from the UV range in which no observable absorbance change was found during the slow decomposition of **2** at the same pH (Table 2). The kinetic studies of the decomposition of **2** were performed at pH < 3. The wavelengths used the decomposition of **2** were 212, 233, and 260 nm.

For **1**, absorbance versus time data were fit to a double exponential rate equation at pH < 3 and to a standard first-order rate equation at pH > 3. For **2**, a standard first-order rate equation was used for data fitting. Two rate constants were observed for the hydrolysis of **1** in solutions with pH < 3. Product yields were monitored by HPLC on the same solutions used for kinetics after 8 half-lives of the hydrolysis reactions. HPLC conditions: 20 μL injections on a 4.7 mm × 250 mm C-8 reverse phase column, 65/

(30) Shi, D.-F.; Bradshaw, T. D.; Wrigley, S.; McCall, C. J.; Lelieveld, P.; Fichtner, I.; Stevens, M. F. G. *J. Med. Chem.* **1996**, *39*, 3375–3384. Bradshaw, T. D.; Wrigley, S.; Shi, D.-F.; Schultz, R. J.; Paull, K. D.; Stevens, M. F. *Br. J. Cancer* **1998**, *77*, 745–752. Bradshaw, T. D.; Shi, D.-F.; Schultz, R. J.; Paull, K. D.; Stevens, M. F. G. *Br. J. Cancer* **1998**, *78*, 421–429. Hutchinson, I.; Chua, M.-S.; Browne, H. L.; Trapani, V.; Bradshaw, T. D.; Westwell, A. D.; Stevens, M. F. G. *J. Med. Chem.* **2001**, *44*, 1446–1455. Hutchinson, I.; Jennings, S. A.; Vishnuvajjala, B. R.; Westwell, A. D.; Stevens, M. F. G. *J. Med. Chem.* **2002**, *45*, 744–747.

(31) Bradshaw, T. D.; Westwell, A. D. *Curr. Med. Chem* **2004**, *11*, 1009–1021. O'Brien, S. E.; Browne, H. L.; Bradshaw, T. D.; Westwell, A. D.; Stevens, M. F. G.; Laughton, C. A. *Org. Biomol. Chem.* **2003**, *1*, 493–497.

(32) Novak, M.; Rajagopal, S. *Adv. Phys. Org. Chem.* **2001**, *36*, 167–253. Novak, M.; Rajagopal, S.; Xu, L.; Kazerani, S.; Toth, K.; Brooks, M.; Nguyen, T.-M. *J. Phys. Org. Chem.* **2004**, *17*, 615–624.

(33) Novak, M.; Chakraborty, M.; Brewer, S. to be submitted.

35 MeOH/H_2O elution solvent, flow rate 1.0 mL/min, monitoring wavelengths = 212, 235 nm.

The isolation of **2**, the hydrolysis product of **1**, was performed in 0.02 M pH 4.61 acetate buffer with concentration of **1** of ca. 7×10^{-4} M. The rate of the decomposition of **2** is negligible at this pH. The procedure for isolation and purification of **2** is described in the synthesis section.

Azide Trapping Studies: Studies of the hydrolysis of **1** in the presence of N_3^- at 80 °C were performed in 0.02 M 1/1 NaH_2PO_4/Na_2HPO_4 buffer (pH 6.6, 5 vol % CH_3CN-H_2O, $\mu = 0.5(NaClO_4)$) at various N_3^- concentrations (0.1, 0.01, 0.008, 0.006, 0.004, 0.002 M). The direct reaction of **2** with N_3^- was negligible under these conditions. Kinetics of the decomposition of **1** in the presence of N_3^- were determined by following the change in the UV absorbance at 310 and 330 nm. Absorbance versus time data were fit to a standard first-order rate equation. The reported rate constant is the average taken at both wavelengths. The yields of products were determined after 2 h reaction time by HPLC using the same conditions as those described above. The yields were determined after 2 h instead of after the completion of the reaction because some of the products decompose slowly in the reaction media. The residual concentration of **1** was monitored by HPLC to ensure that the individual reactions had proceeded to the same extent. Two new HPLC peaks with longer retention time were observed. Only the major adduct was isolated as follows. The ester **1** (50.0 mg, 0.18 mmol), dissolved in 1 mL of CH_3CN, was added in 0.1 mL aliquots every 1 h to 250 mL of a 0.02 M phosphate buffer (pH 6.7, 5 vol % CH_3CN-H_2O, $\mu = 0.5$ ($NaClO_4$)) containing 0.008 M NaN_3 that was incubated in the dark at 80 °C. After the last addition, the mixture was incubated in the dark at 80 °C for an additional 3.5 h. The mixture was then refrigerated overnight and was allowed to reach room temperature before extracting with CH_2Cl_2 (5×50 mL). The combined extract was dried over anhydrous Na_2SO_4, filtered, evaporated to dryness, and subjected to multiple radial chromatography with two solvent systems (5:1 CH_2Cl_2/EtOAc, then 20:1 CH_2Cl_2/CH_3CN). The major azide adduct was separated as a low melting point solid.

4-(6-Azidobenzothiazol-2-yl)phenol (9): IR 3062, 2097, 1606, 1557, 1451, 1435, 1279, 1225, 1168 cm^{-1}; ^1H NMR (500 MHz, DMSO-d_6) δ 6.93 (2H, d, $J = 8.5$ Hz), 7.22 (1H, dd, $J = 8.8$ Hz, 2.3 Hz), 7.91 (2H, d, $J = 8.5$ Hz), 7.93 (1H, d, $J = 2.0$ Hz), 7.97 (1H, d, $J = 8.5$ Hz), 10.22 (1H, s); ^{13}C NMR (125.8 MHz, DMSO-d_6) δ 112.63 (7.93), 116.37 (6.93), 118.66 (7.22), 123.55 (7.97), 124.13, 129.24 (7.90), 136.05, 136.63, 151.59, 160.81, 167.61; LC-MS (ESI, positive) *m/e* 241 $(M - N_2 + H)^+$ (ESI, negative) *m/e* 239 $(M - N_2 - H)^-$; high-resolution MS (ES, positive) $C_{13}H_9N_4OS$ (M + H) calcd 269.0492, found 269.0512.

Steady State Photolysis Experiments. 1. Photolysis: Steady state photolysis of **1** in O_2-saturated pH 5.1, 0.02 M 1/1 acetate buffer (20 vol % CH_3CN-H_2O, $\mu = 0.5$ ($NaClO_4$)) and in O_2-saturated CH_3CN were performed in a Rayonet photochemical reactor in a jacketed quartz vessel kept at 30 °C. Luzchem LZC-UVC lamps that have emission in the range of 235−280 nm were used as the UV source. A brief description of the apparatus for steady state photolysis has been published.[12] Before irradiation, an initial concentration of ca. 6×10^{-4} M of **1** was obtained by adding 5 mL of ca. 0.024 M solution of **1** (33.5 mg, 0.12 mmol) in CH_3CN to 200 mL of O_2-saturated acetate buffer, or by directly adding the ester **1** (33.5 mg, 0.12 mmol) into 200 mL of O_2-saturated CH_3CN. Reaction solutions were mixed thoroughly and then subjected to UV radiation with 1.5−2 min irradiation intervals. The yield of products reached a maximum after ca. 8.5 min of irradiation based on the HPLC analysis that was performed before irradiation and at the end of each irradiation interval (C-8 reverse phase column, 65/35 MeOH/H_2O elution solvent, 1 mL/min, monitored by UV absorbance at 220 and 260 nm). Quantification of products was determined by a combination of HPLC and ^1H NMR of reaction mixtures.

2. Isolation, Purification, and Characterization of Photolysis Products: Photoproducts were isolated from large-scale photolysis of quinol ester **1** in aqueous buffers (primarily **2**, **8**, **11**, **12**, **13**) or in CH_3CN (primarily **8**, **10**, **11**, **13**). The general procedures for product isolation are as follows. For the reactions run in CH_3CN-H_2O mixture, the solution was extracted with CH_2Cl_2 (3×50 mL). The combined extract was dried over anhydrous Na_2SO_4, filtered, and evaporated to dryness. The residue was subjected to further purification as described below. For the reactions run in CH_3CN, photoproducts were subjected to separation and purification directly after removing the solvent by rotary evaporation. An initial separation of photoproducts was performed by radial chromatography on silica gel with 1:1 hexanes/EtOAc. The fractions containing photoproducts were evaporated to dryness under vacuum, and the residues were purified individually by radial chromatography with 9:1 CH_2Cl_2/CH_3CN. Multiple applications of TLC on silica gel with 3:2 hexanes/EtOAc were used to purify **12**. Final purification of **10** and **13** was accomplished by radial chromatography on silica gel with 13:7 hexanes/EtOAc. The peroxy compound **10** decomposes slowly during characterization. Purified products were subjected to HPLC analysis for purity before final characterization. Quinol **2** and the phenols **8** and **11** were identified by direct comparisons to synthesized samples.

4-(Benzothiazol-2-yl)-4-(methylperoxy)cyclohexa-2,5-dienone (10): IR (thin film) 3063, 2924, 1675, 1635, 1612, 1458, 1435 cm^{-1};^1H NMR (500 MHz, DMSO-d_6) δ 3.93 (3H, s), 6.48 (2H, d, $J = 10.2$ Hz), 7.40 (2H, d, $J = 10.1$ Hz), 7.50−7.58 (2H, m), 8.04 (1H, dd, $J = 7.7$ Hz, 0.8 Hz), 8.19 (1H, dd, $J = 8.0$ Hz, 0.9 Hz); ^{13}C NMR (125.8 MHz, DMSO-d_6) δ 64.5, 72.4, 122.6, 123.3, 126.2, 126.8, 130.2, 134.7, 144.7, 151.8, 167.6, 192.7; high-resolution MS (ES, positive) $C_{14}H_{12}NO_3S$ (M + H) calcd 274.0532, found 274.0548.

4-Acetoxy-3-(benzothiazol-2-yl)phenol (12): IR 3233, 3063, 2922, 1757, 1606, 1512, 1432, 1342, 1177, 1108, 1013 cm^{-1}; ^1H NMR (500 MHz, CD_2Cl_2) δ 2.44 (3H, s), 6.99 (1H, dd, $J = 8.7$ Hz, 3.0 Hz), 7.12 (1H, d, $J = 8.7$ Hz), 7.43 (1H, td, $J = 7.5$ Hz, 1.2 Hz), 7.53 (1H, td, $J = 7.7$ Hz, 1.2 Hz), 7.80 (1H, d, $J = 3.0$ Hz), 7.97 (1H, dd, $J = 7.5$ Hz, 0.9 Hz), 8.06 (1H, dd, $J = 7.5$ Hz, 0.6 Hz); ^{13}C NMR (125.8 MHz, CD_2Cl_2) δ 21.85 (2.44), 116.04 (7.80), 118.84 (6.99), 121.85 (7.97), 123.63 (8.06), 125.34 (7.12), 125.86 (7.43), 126.78 (7.53), 127.24, 135.92, 142.45, 153.18, 154.08, 162.32, 169.92; LC-MS (ESI, positive) *m/e* 308 $(M + Na)^+$, 286 $(M + H)^+$, 244 $(M - CH_2CO + H)^+$; (ESI, negative) *m/e* 284 $(M - H)^-$; high-resolution MS (ES, positive) $C_{15}H_{12}NO_3S$ (M + H) calcd 286.0532, found 286.0548.

1,8-Di(benzothiazol-2-yl)-4,5-dioxo-1,4,4a,4b,5,8,8a,8b-octahydrobiphenylene-1,8-diyl diacetate (13): IR 3066, 1764, 1706, 1574, 1436, 1369, 1198, 1179, 1014 cm^{-1}; ^1H NMR (500 MHz, CD_2Cl_2) δ 2.15 (3H, s), 2.92 (1H, d, $J = 5.0$ Hz), 3.88 (1H, dd, $J = 5.0$ Hz, 3.0 Hz), 6.00 (1H, dd, $J = 5.5$ Hz, 1.0 Hz), 7.41 (1H, td, $J = 7.5$ Hz, 5.0 Hz), 7.45 (1H, m), 7.50 (1H, td, $J = 8.2$ Hz, 5.0 Hz), 7.88 (1H, d, $J = 8.0$ Hz), 7.96 (1H, d, $J = 8.0$ Hz); ^{13}C NMR (125.8 MHz, CD_2Cl_2) δ 20.76 (2.15), 37.14 (2.92), 37.81 (3.88), 77.96, 122.10 (7.88), 123.56 (7.96), 125.89 (7.41), 126.87 (7.50), 132.93(6.00), 135.10, 153.29, 153.90, 168.08, 170.66, 199.79; LC/MS (ESI, positive) *m/e* 593 $(M + Na)^+$, 308 $(M/2 + Na)^+$, 286 $(M/2 + H)^+$, 249 $(M/2 - OAc + Na)^+$; high-resolution MS (ES, positive) $C_{30}H_{22}N_2O_6S_2Na$ (M + Na) calcd 593.0811, found 593.0839.

Synthesis. 4-(Benzothiazol-2-yl)phenol (8):[34] 4-Hydroxybenzaldehyde (3.66 g, 23 mmol) and 2-aminothiophenol (7.51 g, 60 mmol) were dissolved in 100 mL of Et_2O. Silica gel (30 g) was added to the mixture, and the solvent was slowly evaporated under vacuum. The dry mixture was divided into four portions, placed into four sealable Teflon vessels, and subjected to microwave heating at a maximum power of 650 W for 3 min. The silica gel

(34) Kodomari, M.; Tamaru, Y.; Aoyama, T. *Synth. Commun.* **2004**, *34*, 3029–3036.

was washed with 9:1 hexanes/EtOAc (4 × 50 mL), EtOAc (4 × 50 mL), and EtOH (4 × 50 mL). Silica gel (15 g) was added to the EtOAc wash again, and the solvent was removed. The dry residue was washed again with 9:1 hexanes/EtOAc (2 × 50 mL), EtOH (2 × 50 mL), followed by hot EtOH (1 × 50 mL). The hexanes/EtOAc washes were discarded. All the EtOH filtrates were combined and evaporated to dryness under vacuum to yield crude **8**. A clean sample of **8** was obtained by recrystallization from EtOH: mp 226.5−227.5 °C, lit[34] mp 227 °C; ^{1}H NMR (300 MHz, DMSO-d_6) δ 6.93 (2H, d, J = 8.5 Hz), 7.39 (1H, td, J = 7.5 Hz, 1.2 Hz), 7.49 (1H, td, J = 7.7 Hz, 1.2 Hz), 7.92 (2H, d, J = 8.7 Hz), 7.97 (1H, d, J = 7.8 Hz), 8.07 (1H, d, J = 7.8 Hz), 10.21 (1H, s); ^{13}C NMR (125.8 MHz, DMSO-d_6) δ 116.04, 122.05, 122.25, 124.01, 124.84, 126.36, 128.99, 134.07, 153.69, 160.48, 167.40.

4-(Benzothiazol-2-yl)-2-methylphenol (11): This compound was synthesized from 4-hydroxy-3-methylbenzaldehyde and 2-aminothiophenol as described above for **8**. The crude product was purified by recrystallization from EtOH: mp 229−230 °C; IR 3061, 2923, 1601, 1401, 1277, 1120 cm^{-1}; ^{1}H NMR (500 MHz, DMSO-d_6) δ 2.21 (3H, s), 6.93 (1H, d, J = 8.5 Hz), 7.38 (1H, td, J = 7.6 Hz, 1.3 Hz), 7.49 (1H, td, J = 7.6 Hz, 1.2 Hz), 7.75 (1H, dd, J = 8.3 Hz, 2.3 Hz), 7.83 (1H, d, J = 1.5 Hz), 7.95 (1H, d, J = 7.5 Hz), 8.06 (1H, d, J = 7.5 Hz), 10.12 (1H, s); ^{13}C NMR (125.8 MHz, DMSO-d_6) δ 15.81 (2.21), 115.11 (6.93), 122.04 (8.06) 122.17 (7.95), 123.83, 124.77 (7.38), 124.99, 126.34 (7.49), 126.44 (7.75), 129.59 (7.83), 134.05, 153.70, 158.68, 167.58; LC/MS (ESI, positive) *m/e* 242 (M + H)$^+$, (ESI, negative) *m/e* 240 (M − H)$^-$; high-resolution MS (ES, positive) $C_{14}H_{12}NOS$ (M + H) calcd 242.0634, found 242.0644.

4-Acetoxy-4-(benzothiazol-2-yl)-2,5-cyclohexadien-1-one (1): **8** (0.455 g, 2 mmol) was dissolved in 30 mL of AcOH, and the resulting solution was stirred and kept in a water bath at 30−33 °C as a solution of PIDA (0.708 g, 2.2 mmol) in 15 mL of AcOH was added dropwise over a period of 1.5 h. The reaction solution was stirred for another 30 min at room temperature after completion of the addition. AcOH was removed by rotary evaporation under vacuum, and the residue was left on the vacuum pump overnight. The dry residue was dissolved in ca. 25 mL of EtOAc followed by filtration. The filtrate was collected and evaporated to dryness and then subjected to trituration with hot 75/25 hexanes/EtOAc. The solvent was removed, and oily yellow **1** was obtained. Further purification was performed by multiple application of radial chromatography on silica gel with 2:1 hexanes/EtOAc (yield 10−20%): mp 98−100 °C; IR 3065, 3050, 2930, 1751, 1668, 1629, 1432, 1370, 1214, 1163, 1040 cm^{-1}; ^{1}H NMR (300 MHz, DMSO-d_6) δ 2.19 (3H, s), 6.43 (2H, d, J = 10.2 Hz), 7.36 (2H, d, J = 9.9 Hz), 7.47−7.52 (2H, m), 8.02 (1H, dd, J = 7.8 Hz, 1.5 Hz), 8.16 (1H, dd, J = 7.5 Hz, 1.5 Hz); ^{13}C NMR (75.5 MHz, DMSO-d_6) δ 20.46, 75.66, 121.85, 122.76, 125.50, 126.18, 128.60, 134.22, 144.38, 151.89, 166.83, 167.90, 184.02; high-resolution MS (ES, positive) $C_{15}H_{12}NO_3S$ (M + H) calcd 286.0532, found 286.0549, $C_{15}H_{11}NO_3SNa$ (M + Na) calcd 308.0352, found 308.0370.

4-(Benzothiazol-2-yl)-4-hydroxy-2,5-cyclohexadien-1-one (2): **2** was obtained from hydrolysis of **1**. The procedure is as follows: 250 mL of 0.02 M, 1/1 AcOH/AcONa buffer (pH 4.61 5 vol % CH_3CN, μ = 0.5 ($NaClO_4$)) was prepared and incubated in a water bath at 80 °C prior to the addition of **1**. A freshly made solution of **1** (50 mg, 0.175 mmol) in 1 mL of CH_3CN was added in 0.1 mL aliquots every 1 h to the incubated acetate buffer over a period of 10 h. After the last addition, the reaction mixture was kept in the dark at 80 °C for another 5 h before refrigerating overnight. It was brought back to room temperature the next day and extracted with CH_2Cl_2 (5 × 50 mL). The combined CH_2Cl_2 extract was dried over anhydrous Na_2SO_4, filtered, and evaporated to dryness under vacuum. The crude product was purified by radial chromatography with 3:2 hexanes/EtOAc (yield 71%): mp 108−109.5 °C, lit[2] mp 63−66 °C; IR 3168, 1674, 1607, 1494, 1434, 1386, 1147, 1069, 1055 cm^{-1}; ^{1}H NMR (300 MHz, CD_2Cl_2) δ 4.35 (1H, s), 6.32 (2H, d, J = 9.9 Hz), 7.01 (2H, d, J = 9.9 Hz), 7.42−7.55 (2H, m), 7.93 (1H, dd, J = 8.7 Hz, 0.6 Hz), 8.01 (1H, dd, J = 8.5 Hz, 0.8 Hz); ^{13}C NMR (75.5 MHz, CD_2Cl_2) δ 71.76, 122.68, 124.06, 126.55, 127.24, 129.37, 136.82, 148.04, 153.51, 171.45, 185.00; high-resolution MS (ES, positive) $C_{13}H_{10}NO_2S$ (M + H) calcd 244.0427, found 244.0439.

Calculations: Density functional calculations were carried out using the Gaussian 03 suite of programs.[35] Geometry optimization of the ground state oxenium ions **3** and **5a** and the quinols **2**, **7a**, and **7b** were executed at the B3LYP/6-31G(d) level, and their verification as a minimum and derivation of IR vibrational frequencies and normal modes of vibration were executed using a harmonic frequency analysis, which afforded all real frequencies. Calculations at this level were previously reported for **5b**.[13] Vibrational frequencies for comparison with experimental data were scaled by a factor of 0.9614 according to Scott and Radom.[18]

Acknowledgment. We thank the Donors of the American Chemical Society Petroleum Research Fund (Grant # 43176-AC4) for partial support of this work. Y.-T.W. thanks the Department of Chemistry and Biochemistry at Miami University for a Dissertation Fellowship, and K.J.J. thanks Miami University for an Undergraduate Summer Scholars Award and an Undergraduate Research Award.

Supporting Information Available: Table S1, containing all rate constants collected for **1** and **2**; Tables S-2−S-10, containing the *Z*-matrices for the optimized structures of singlet (S_o) **2**, **3**, **5a**, **7a**, **7b**, and 2-methylbenzothiazole and triplet (T_1) **3**, **5a**, and **5b** at the B3LYP/6-31G(d) level of theory; ^{1}H and ^{13}C NMR spectra for **1**, **2**, **9**, **10**, **11**, **12**, and **13**; and complete ref 35. This material is available free of charge via the Internet at http://pubs.acs.org.

JO9008436

(35) Frisch, M. J.; et al. *Gaussian 03*, revision E.01; Gaussian, Inc.: Wallingford, CT, 2005.